Desalination and Water Treatment
www.deswater.com

1944-3994/1944-3986 © 2011 Desalination Publications. All rights reserved
doi: 10/5004/dwt.2011.2197

28 (2011) 35–41
April

Aqueous phase adsorption of organic compounds on activated carbon in fluidized bed

Esmail Rezaei[a], Omid Mowla[b], Dariush Mowla[c,*]

[a]*Shiraz Petrochemical Complex, Marvdasht, Iran*
[b]*Civil and Environmental Engineering Department, Shiraz University, Shiraz, Iran*
[c]*Environmental Research Centre in Oil, Gas and Petrochemical Industries, Shiraz University, Shiraz, Iran*
Tel. +98 711 6133764; email: dmowla@shirazu.ac.ir

Received 1 February 2009; Accepted 1 July 2010

ABSTRACT

In this study, the adsorption of an organic compound in aqueous phase on granular activated carbon (GAC) in a liquid fluidized bed has been studied. For this purpose first a mathematical model was proposed for simulation of this process. Based on the proposed model, the adsorption kinetic and dynamic simulation of organic compounds on activated carbon were investigated. In order to check the accuracy of the proposed model, an experimental set-up was constructed. This set-up was consisted of a feed tank, a pump, a flow meter and a liquid fluidized bed absorber column. In this set up, some experiments were conducted for adsorption of methyl-orange solution on AC particles. The results obtained by the proposed model were compared with the experimental results and once the validity of the model was verified, it was used for studying the effect of different operating parameters on the rate of adsorption in such beds.

Keywords: Surface adsorption; Fluidized bed; Granular activated carbon; Adsorption kinetics; Mathematical model

1. Introduction

Liquid organic compounds have been extensively used as important ingredients and many of them have been used as solvents in wide variety of manufacturing processes. The environmental problems associated with these organic compounds stem mainly from the presence of these compounds in wastewater in low concentration. A large number of these organic compounds have serious health consequences and some of them are cancer causing. Hence removal of these organic compounds has become increasingly important and in many cases urgently needed [1].

Activated carbon adsorption has been widely considered as a potential treatment for removing organic matters from wastewater as it has a strong affinity for adsorption of organic substances even at low concentration [1–3].

Granular activated carbon (GAC) is the most effective absorbent for organic contaminants due to its high specific surface, low cost and fast adsorption kinetics [3,4].

This work addresses the adsorption of an organic compound in granular activated carbon fluidized bed under a wide range of operating conditions with a combination of experimental and modeling studies. The processes dynamic was described using a model that considers external film diffusion followed by intra particle surface diffusion with a surface diffusion coefficient that increases exponentially with surface coverage [5,6].

In liquid–solid systems, an increase in flow rate above minimum fluidization usually results in a smooth, progressive expansion of the bed. Gross flow instabilities are damped and remain small, and heterogeneity, or large-scale voids of liquids, are not observed under normal conditions. A bed such as this is called a homogeneously fluidized bed. In this case the velocity of liquid is between

---

*Corresponding author.

Presented at the 1st International Conference on Water and Wastewater Treatment, April 21–22, 2010, Isfahan, Iran

minimum fluidization velocity and carry over velocity of particles by the liquid [7].

A large number of experimental and modeling studies have been previously reported on the adsorption of organic compounds from aqueous solutions on activated carbon. Activated carbon adsorption from aqueous solution is most commonly described by use of the homogeneous surface diffusion model [5,6,8–11,14].

2. Mathematical modeling

In the proposed model, the adsorbent particles are assumed to be spherical and isotropic with uniform pores and no preferential pore direction. The solute diffuses through the boundary layer surrounding the adsorbent particles and is adsorbed on their external surface. Diffusion inside the particle is assumed to take place only on the pore walls (surface diffusion) with the contribution of pore diffusion being assumed as negligible.

The surface diffusion coefficient was assumed to increase exponentially with surface coverage according to the following expression [5,6]:

$$D_s = D_0 \exp\left[K\frac{C_{ss}}{Css,\,eq}\right] \tag{1}$$

Eq. (1) was used to allow for both a concentration independent ($K=0$) and a concentration dependent D_S ($K\neq 0$). Other assumptions involved in the model include isothermal conditions and fast intrinsic adsorption kinetics, resulting in equilibrium between the solid-phase and liquid-phase solute concentrations at the external surface of the particles.

The solute diffusion inside a spherical adsorbent particle is described by the following equation:

$$\frac{\partial C_{ss}}{\partial t} = \frac{1}{r^2}\frac{\partial}{\partial r}\left[r^2 D_s \frac{\partial C_{ss}}{\partial r}\right] \tag{2}$$

Combining Eqs. (1) and (2) will result in the following equation [8,9]:

$$\frac{\partial C_{ss}}{\partial t} = \frac{D_0}{r^2}\frac{\partial}{\partial r}\left[r^2 \exp\left(K\frac{C_{ss}}{C_{ss,sat}}\right)\frac{\partial C_{ss}}{\partial r}\right] \tag{3}$$

With the following initial and boundary conditions [5,6,8–11]:

$$\text{IC:}\quad t<0 \quad C_{ss}=0 \quad 0\le r\le r_0$$

$$\text{BC1:}\quad t>0 \quad \left.\frac{\partial C_{ss}}{\partial r}\right|_{r=0} = 0$$

$$\text{BC2:}\quad t>0 \quad D_0\rho_p \exp\left[K\left(\frac{C_{ss}}{C_{ss,sat}}\right)\right]\left.\frac{\partial C_{ss}}{\partial r}\right|_{r=r_0} = K_f\,(C-C_s)$$

In the absence of axial solute dispersion in the bed, the solute mass balance in the liquid phase along with the relevant IC and BCs is given as

$$\frac{\partial C}{\partial t} = -\frac{U_b}{\varepsilon}\frac{\partial C}{\partial z} - K_f\frac{3(1-\varepsilon)}{\varepsilon r_0}(C-C_s) \tag{4}$$

$$\text{IC:}\quad t\le 0 \quad C=0 \quad 0\le z\le L$$

$$\text{BC:}\quad t>0 \quad C=C_0 \quad z=0$$

Petrovic and Thodos showed that K_f the mass transfer coefficient in liquid fluidized beds is given as follows [13]:

$$StSc^{2/3} = \frac{K_f}{U}\varepsilon Sc^{2/3} = 0.81\left(\frac{Ud_p\rho_f}{\mu}\right)^{-0.5} \tag{5}$$

$$5 < \frac{Ud_p\rho_f}{\mu} < 500, \quad 100 < SC < 1000,$$

$$0.43 < \varepsilon < 0.63$$

$$StSc^{2/3} = \frac{K_f}{U}\varepsilon Sc^{2/3} = 0.6\left(\frac{Ud_p\rho_f}{\mu}\right)^{-0.43} \tag{6}$$

$$50 < \frac{Ud_p\rho_f}{\mu} < 200, \quad 0.6 < SC < 2000,$$

$$0.43 < \varepsilon < 0.75$$

At the solid–liquid interface, the solute concentrations in solid-phase and liquid-phase are related through the equilibrium isotherm. For Freundlich isotherm they are related as follows [5,6,15,16]:

$$\left.C_{ss}\right|_{r=r_0} = K_L C_s^n \tag{7}$$

Using the following dimensionless quantities [5,6]:

$$\rho = \frac{r}{r_0}, \quad \xi = \frac{z}{L}, \quad U = \frac{C}{C_0},$$

$$U_s = \frac{C_s}{C_0}, \quad \eta = \frac{C_{ss}}{C_{ss,0}}$$

$$Bi = \frac{K_f r_0 C_0}{\rho_p D_0 C_{ss,0}}, \quad \tau = \frac{D_0 t}{r_0^2}, \quad A = \frac{U_b r_0^2}{D_0 L_\varepsilon},$$

$$B = \frac{3(1-\varepsilon)K_f r_0}{D_0\varepsilon}$$

Eqs. (3), (4) and (7) can be rendered dimensionless as follows:

$$\frac{\partial\eta}{\partial\tau} = \frac{1}{\rho^2}\frac{\partial}{\partial\rho}\left[\rho^2\exp\left(K\frac{\eta}{\eta_{sat}}\right)\frac{\partial\eta}{\partial\rho}\right]$$

$$\text{IC:}\quad t<0 \quad \eta=0 \quad 0\le\rho\le 1 \tag{8}$$

$$\text{BC1:}\quad \tau>0 \quad \left.\frac{\partial\eta}{\partial\rho}\right|_{\rho=0} = 0$$

$$\text{BC2:}\quad \tau>0 \quad \left.\frac{\partial\eta}{\partial\rho}\right|_{\rho=1} = Bi(U-U_S)$$

$$\frac{\partial U}{\partial \tau} = -A\frac{\partial U}{\partial \xi} - B(U - U_S) \tag{9}$$

$$\begin{array}{llll} \text{IC:} & \tau < 0 & U = 0 & 0 \le \zeta \le 1 \\ \text{BC:} & \tau > 0 & U = U_0 & \zeta = 0 \end{array}$$

$$\eta|_{\rho=1} = U_S^n \tag{10}$$

The adsorption kinetic coefficients D_0 and K of Eq. (1) are determined by solving the partial differential Eqs. (8), (9) and algebraic Eq. (10) simultaneously. These equations are written in finite difference form and solved by an implicit method assuming $K = 0$. As a result, D_S is calculated at specific time intervals. At the same time intervals, the exit solution concentration of organic compound from the fluidized bed column could be obtained. Therefore, D_S is determined as a function of organic adsorbate concentration on activated carbon. Adsorption coefficient can be estimated using a nonlinear regression method such as Marquardt's.

In the adsorption simulations, Eqs. (8–10) are written in finite difference form and solved by an implicit method (Crank–Nicholson) with assuming $K \neq 0$.

3. Materials and methods

3.1. Materials

Methyl-orange (4-dimethylaminoazobenzene-4′-sulfonic acid sodium salt) was selected as an organic compound or dye that its concentration in aqueous solution is measured using a UV-spectrophotometer at 467 nm.

Coconut charcoal with the specification as shown in Table 1 was selected as an activated carbon for adsorbing of methyl-orange.

3.2. Adsorption isotherm

The equilibrium isotherm for methyl-orange adsorption from an aqueous solution on coconut activated carbon was determined at 27 °C. Before each set of experiments, the activated carbon was repeatedly rinsed with DM water to remove the fines, dried overnight at 110 °C and stored in desiccators [5,6,9,10].

Table 1
Coconut charcoal specification

Mesh size	Absolute density ρ_{true} (g/cm^3)	Particle density ρ_p (g/cm^3)	Porosity x
8–12	1.68	0.9	0.464
12–16			
16–20			

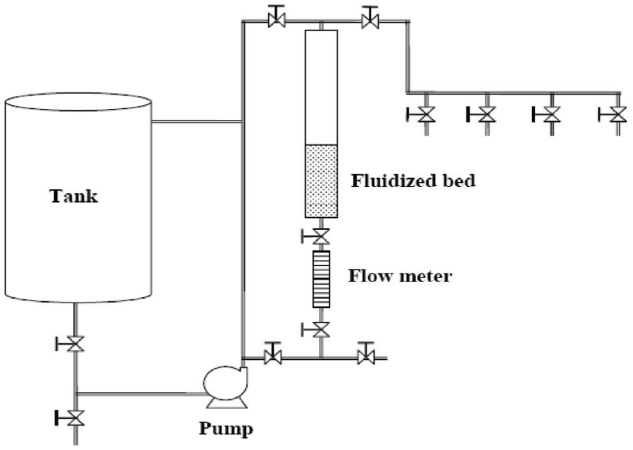

Fig. 1. Schematic diagram of the experimental setup.

Five samples of activated carbon with different weights were poured into five glass bottles (0.25 l). Then the bottles were filled with methyl-orange solution (200 ml, 300 mg/l) and shacked continuously for 7 d after which equilibrium is assumed to be achieved. After this time period, the amount of methyl-orange adsorbed per unit mass of AC, $C_{SS,eq}$ (mg/l) , was calculated by the following equation [1,3,6,8,9,12,16].

$$C_{SS,eq} = \frac{V(C_i - C_{eq})}{W} \tag{11}$$

where C_i (mg/l) and C_{eq} (mg/l) are the concentrations of the methyl-orange in the solution at initial and equilibrium conditions respectively. V (l) is the volume of the organic solution, and W (g) is the mass of AC used. In order to avoid any vaporization during the experiment, the bottles were covered by Teflon caps.

3.3. Fluidized bed adsorption

Aqueous phase adsorption of methyl-orange on AC particles was conducted in a liquid fluidized bed column of 2.85 cm diameter under different operating conditions of AC particle size, inlet solution concentration and inlet solution flow rate. A schematic diagram of the experimental setup used is shown in Fig. 1.

4. Result and discussion

4.1. Adsorption isotherm data

The adsorption equilibrium data were fitted with several well-known isotherm models using Marquardt–Levenberg optimization procedure to minimize the root

Table 2
Parameters values from fitting the adsorption equilibrium data with various isotherms models

	Isotherm model	Parameter value RMS (%)	Normalized
(1) Langmuir	$C_{SS,eq} = \dfrac{K_L q^\circ C_{eq}}{1 + K_L C_{eq}}$	$q^0 = 68.10304$ $K_L = 1.786$	11.2605
(2) Freundlich	$C_{SS,eq} = K_L C_{eq}^{nf}$	$K_L = 43.11434$ nf=0.16481	2.4013
(3) Radke–Prausnits	$C_{SS,eq} = \dfrac{a_1 a_2 C_{eq}}{1 + a_2 C_{eq}^{b}}$	$a_1 = 44.38179$ $a_2 = 33.0004$ $b = 1.84453$	2.4449
(4) Toth	$C_{SS,eq} = \dfrac{K_T q_T C_{eq}}{[1 + (K_T C_{eq})^n]^{1/n}}$	$K_T = 84.46094$ $q_T = 113.37416$ $n = 0.26877$	4.1935
(5) Fritz–schlunder	$C_{SS,eq} = \dfrac{\alpha_1 C_{eq}^{\beta_1}}{1 + \alpha_2 C_{eq}^{\beta_2}}$	$\alpha_1 = 131.19968$ $\alpha_2 = 2.06813$ $\beta_1 = 0.02855$ $\beta_2 = 0.23468$	2.3559

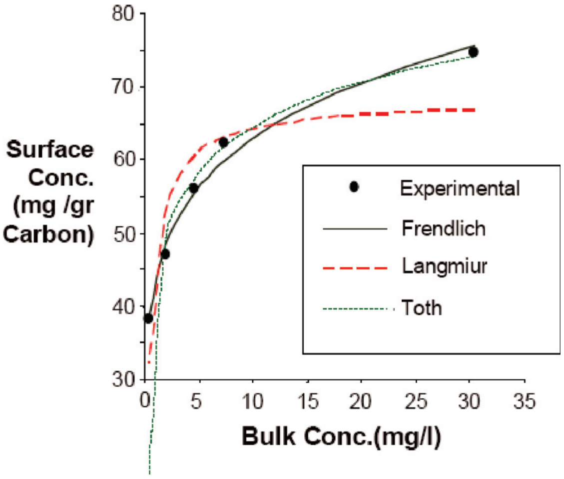

Fig. 2. Experimental aqueous-phase adsorption isotherm for methyl-orange/coconut charcoal system.

mean square of the normalized residuals between the experimental and computed concentrations defined as follows [5,6]:

$$\text{Normalized RMS} = 100\sqrt{\frac{1}{N}\sum_{i=1}^{N}\left(\frac{C_{SS,eq,i}^{exp} - C_{SS,eq,i}^{cal}}{C_{SS,eq,i}^{exp}}\right)^2} \qquad (12)$$

The results of the fitting procedure are presented in Table 2.

Fig. 2 shows the experimental aqueous-phase adsorption isotherm for methyl-orange/coconut activated carbon system at 27 °C along with the curves fitted by Langmuir, Freundlich and Toth isotherm models.

As it is observed from this figure the Langmiur isotherm gives the poorest fit and Freundlich and Fritz–Schlunder isotherms give the best fit. Freundlich equation is selected in this study due to its convenience in calculations.

4.2. Adsorption rate data

At initial steps of adsorption, the concentration dependence of the surface diffusion coefficient D_S was ignored (i.e., $D_S = D_0$, $K = 0$ in Eq. (1)). Eqs. (8)–(10) were solved simultaneously and D_S was calculated in specific time intervals. A set of experiments was conducted for determining exit solution concentration from fluidized bed at these time intervals. The obtained experimental and calculation data are shown in Table 3.

The absorbed amount of methyl-orange per unit mass of activated carbon $C_{SS,t}$ (mg/g) was calculated as

$$C_{SS,t} = \frac{V(C_0 - C_{ext})}{W} \qquad (13)$$

where C_0 (mg/l) is the inlet concentration and C_{ext} (mg/l) is the exit concentration of methyl-orange from fluidized bed. V (l) is the volume of the organic solution flowing through the bed and W (g) is the mass of dry absorbent used.

Therefore values of D_S are obtained as a function of methyl-blue concentration on activated carbon. Adsorption kinetic and coefficients (D_0, K) of Eq. (1) are determined by nonlinear regression between the D_0 values and the absorbed amount of absorbate ($C_{SS,t}$):

$D_0 = 6.85 \times 10^{-10}$ cm²/s, $K = 1.7$

Table 3
Experimental and calculated data for determining surface diffusion coefficients

Time (min)	C (mg/l)	V (l)	C_{ext} (mg/l)	$C_{SS,t}$ (mg/gr carbon)	D_0 (cm²/s)
30	20.196	15.15	19.522	2.258	8.56 × 10–11
60	20.603	30.30	19.987	4.351	7.16 × 10–10
90	20.925	45.45	20.356	5.688	1.66 × 10–9
120	21.111	60.60	20.683	6.593	3.81 × 10–9

W = 20 gr, C_0 = 22.589 mg/l, Q = 30.3 l/h, $d_p \approx$ 0.0912 cm

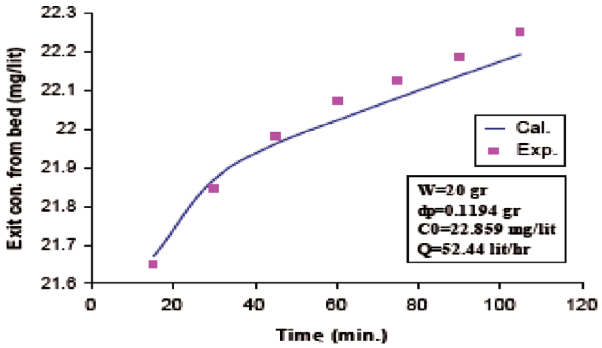

Fig. 3. Experimental adsorption rate curve with the model prediction.

In order to verify the ability of the proposed model to describe the rate of adsorption under other operating conditions, some additional experiments were conducted using two other inlet concentrations, two other inlet liquid velocities and two other activated carbon particle sizes. One of the experimental adsorption rate curves is shown together with the model prediction in Fig. 3. It is evident from this figure that the model prediction is good enough, confirming the ability of the proposed model to (homogeneous surface diffusion model) to successfully describe the process with the set of parameters previously obtained.

So the proposed model could be used to investigate the effects of initial solution concentration, inlet volumetric flow rate and particle size of activated carbon on the rate of adsorption of methyl-orange on activated carbon in a fluidized bed absorber as follows.

4.3. Effect of the inlet solution concentration

The inlet concentration of the organic compounds is one of the main parameters in adsorption process. The breakthrough curve for this effect is presented in Fig. 4.

Increasing the inlet organic concentration at constant flow rate, increases the slope of breakthrough curve. This may be caused by more quickly saturation of the adsorbent for high inlet organic concentration, therefore decreasing the breakthrough time.

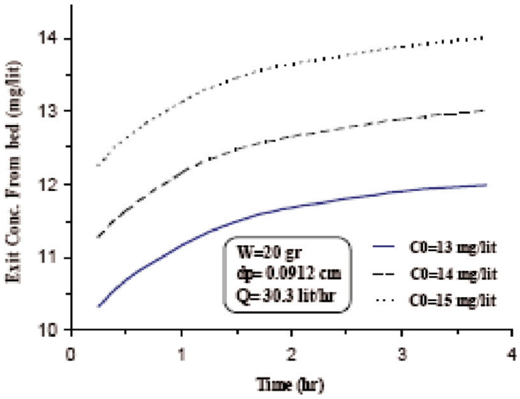

Fig. 4. Breakthrough curve for various initial concentrations.

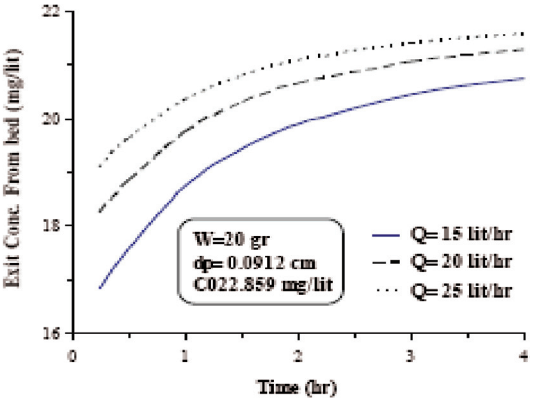

Fig. 5. Breakthrough curve for various inlet solution flow rate.

4.4. Effect of the inlet solution volumetric flow rate

The effect of the inlet solution volumetric flow rate was investigated and the breakthrough curve is presented in Fig. 5 for this case.

From Fig. 5, it is obvious that decreasing of the solution volume flow rate will increase the slope of the breakthrough curve. This is due to the increased contact time between the organic solution and adsorbent at lower flow rates.

4.5. Effect of the particle size of activated carbon

The effect of the activated carbon particle size on the adsorption rate of organic compounds was investigated and its breakthrough curve is presented in Fig. 6.

Decreasing the adsorbent particle size at constant volume flow rate and inlet solution concentration, increases the contact surface area between aqueous solution of organic compound and adsorbent. Therefore, increases the slope of breakthrough curve and the rate of adsorption.

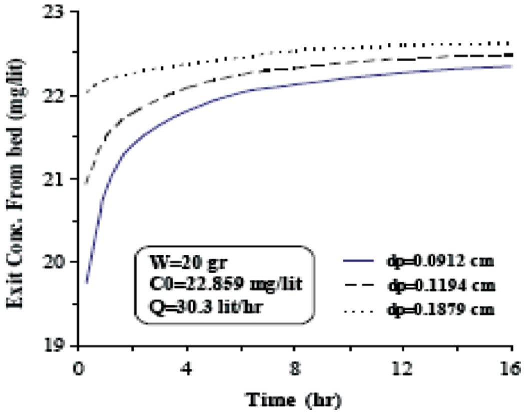

Fig. 6. Breakthrough curve for various particle sizes.

5. Conclusion

The aqueous adsorption of an organic compound (methyl-orange) on granular coconut activated carbon in a fluidized bed column was studied. The experimental results showed that coconut activated carbon could remove this organic compound effectively. The effects of the different operating variables such as inlet solution flow rate, inlet organic concentration and activated carbon particle size were studied in this system.

Adsorption processes were described using a model that considers external film diffusion followed by intra particle surface diffusion with a surface diffusion coefficient that increases exponentially with surface coverage. The results given by the proposed model are in good agreement with those obtained experimentally. The following results are obtained from this study:

(a) Increasing the inlet solution concentration increases the slope of breakthrough curve and adsorption rate.
(b) Decreasing the inlet flow of solution increases the slope of the breakthrough curve and rate of adsorption.
(c) Decreasing the particle size of activated carbon increases the slope of the breakthrough curve and rate of adsorption.

Symbols

C — Solute liquid phase concentration (m/l)
C_{SS} — Solute surface (solid-phase) concentration (mg/g)
D — Solute diffusion coefficient in the liquid phase (cm²/s)
D_0 — Surface diffusion coefficient at $C_{SS} = 0$ (cm²/s)
D_S — Surface diffusion coefficient (cm²/s)
R — Radial position inside the absorbent particle (cm)
t — Time (s)
z — Axial position in bed (cm)
U_b — Superficial liquid velocity in bed (cm/s)
r_0 — Absorbent particle radius (cm)
K_L — Freundlich constant
K_f — External mass transfer coefficient (cm/s)
K — Parameter defined in Eq. (1)
V — Solution volume (l)
W — Activated carbon mass (g)
C_i — Initial solute concentration (mg/g)
C_{eq} — Equilibrium solute concentration
n — Exponential parameter
ρ_p — Particle density (g/cm³)
Sc — Schmidt number
U — Dimensionless solute liquid-phase concentration
L — Length of fluidized bed (cm)

Greeks

ε — Fluidized bed porosity
η — Dimensionless solute surface concentration
ζ — Dimensionless axial position in bed
ρ — Dimensionless solute liquid-phase concentration
α — Particle porosity

Subscripts

i — Initial value at $t = 0$
cal — Calculated
eq — Equilibrium
exp — Experimental
0 — Bed inlet $z = 0$
s — Particle–liquid interface $r = r_0$
sat — Surface saturation

References

[1] H. Sheng and M. Feng, Liquid-phase adsorption of organic compounds by granular activated carbon and activated carbon fiber, Ind. Eng. Chem. Res., 34 (1995) 2110–2116.
[2] A.H. Roy, Activated carbon system for separation of liquids, Hand Book of Separation Technique for Chemical Engineering, (1997) 1587–1618.
[3] W. Xing, H.H. Ngo, S.H. Kim, W.S. Guo and P. Hagare, Adsorption and bioadsorption of granular carbon (GAC) for dissolved organic carbon (DOC) removal in wastewater, Biores. Tecnol., (2008).
[4] E. Sabio, F. Zamora, J. Ganan, C.M. Gonzalez-Garcia and J.F. Gonzalez, Adsorption of *p*-nitro phenol on activated carbon fixed bed, Water Res., 40 (2009) 3053–3060.

[5] Ch. Dimitrios and V. Arvind, Aqueous-phase adsorption and desorption of toluene in activated carbon fixed bed: experiments and model, Chem. Eng. Sci., 50(1) (1995) 127–141.

[6] Ch. Dimitrios and V. Arvind, Activated carbon adsorption and desorption of toluene in aqueous phase, AICHE J., 39 (1993) 2027–2041.

[7] Daizo Kunii and Octav Levenspiel, Fluidization Eng., (1969).

[8] H.W. Lee and K.J. Kim, Removal of phenol by adsorption powdered activated carbon in a continuous flow stirred cell membrane system, Sep. Sci. Technol., 32(11) (1997) 1835–1849.

[9] M. Mamdouh and H. Yehia, Removal of different basic dyes from aqueous solution by adsorption on Palm-Fruit Banch particle, Chem. Eng. J., 66 (1997) 223–226.

[10] B. Al-Duri and G. Mckay, Multicomponent dye adsorption onto carbon using a solid diffusion mass transfer model, Ind. Eng. Chem. Res., 30 (1991) 385–395.

[11] I. Neretnieks, Adsorption finite batch and counter current flow with system having nonlinear isotherm, Chem. Eng. Sci., 31 (1976) 107–114.

[12] L. Jossens and J. Prausnitz, Thermodynamic of multi-solute adsorption from dilute aqueous solution, Chem. Eng. Sci., 33 (1978) 1097–1106.

[13] J.F. Davidson and D. Harrison, Fluidization, 1977.

[14] L. Markovska, V. Meshko, V. Noveski and M. Marinkovski, Solid diffusion control of adsorption of basic dyes onto granular activated carbon and natural zeolite in fixed bed column, J. Serb. Chem. Soc., 66(7) (2001) 463–475.

[15] L. Peereboom, B. Koenigsknecht, M. Hunter, J.E. Jackson and D.J. Miller, Aqueous phase adsorption of glycerol and propylene glycol onto activated carbon, Carbon, 45 (2007) 579–586.

[16] S.G. Reznik, I. Katz and C.G. Dosoretz, Removal of dissolved organic matter by granular activated carbon adsorption as a pretreatment to reverse osmosis of membrance bioreactor effluents, Water Res., 42 (2008) 1595–1605.